k-dependent electronic structure of the colossal magnetoresistive perovskite La$_{0.66}$Sr$_{0.34}$MnO$_3$

M. Shi,[1] M. C. Falub,[1] P. R. Willmott,[1,2] J. Krempasky,[1] R. Herger,[1,2] K. Hricovini,[3] and L. Patthey[1]

[1]*Swiss Light Source, Paul Scherrer Institute, CH-5232 Villigen PSI, Switzerland*
[2]*Physical Chemistry Institute, University of Zurich, CH-8057 Zurich, Switzerland*
[3]*Université de Cergy-Pontoise, 95031 Cergy-Pontoise CEDEX, France*

We present the first angle-resolved photoemission spectroscopy (ARPES) results on three-dimensional manganese perovskite La$_{0.66}$Sr$_{0.34}$MnO$_3$. In contrast to ARPES results on layered manganites, a finite and *k*-dependent spectral weight at the Fermi level was observed. We propose a complex energy band to describe the low binding energy electronic states, which may result from the temporally dynamic orbital orientation distributions and/or nanoscale charge inhomogeneities, to account for the anomalously broad ARPES features observed in the measurements. Flat sections of the Fermi surface were determined. A density wave resulting from nesting instabilities induced by the flat Fermi surface sections is manifested by the energy band folding.
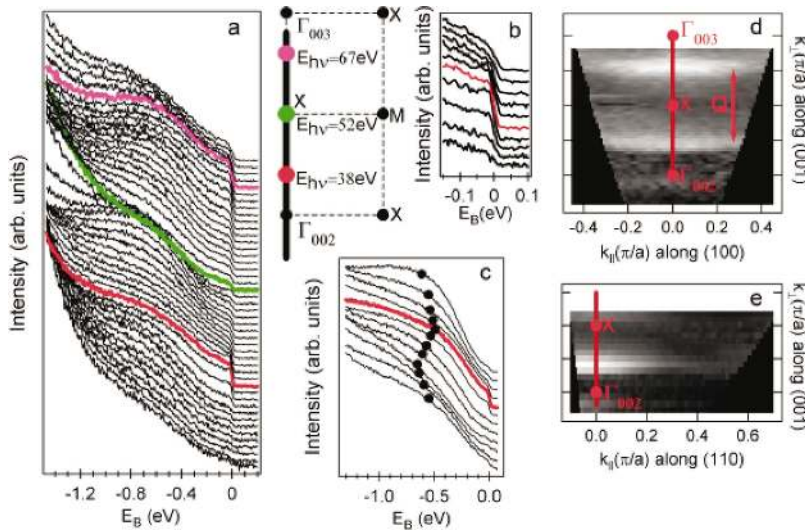
The discovery of colossal magnetoresistance in hole-doped manganese oxides with perovskites structure has stimulated considerable interest in understanding the electronic and magnetic properties of these materials.[1,2] As a model system, La$_{1-x}$Sr$_x$MnO$_3$ has a very rich phase diagram.[3,4] Within a certain range of doping, it shows a large decrease in resistivity upon cooling, associated with a paramagnetic (PM) to ferromagnetic (FM) transition. Close to the transition temperature T_c, the resistivity can be further strongly reduced by applying a magnetic field, known as colossal magnetoresistance (CMR). In the FM phase La$_{1-x}$Sr$_x$MnO$_3$ is a mixed valent with Mn^{3+} and Mn^{4+}. For the site symmetry of the cation in the MnO$_6$ octahedra, the valence states in question are Mn^{4+}:$t_{2g}{}^3$ and Mn^{3+}:$t_{2g}{}^3$ $e_g{}^1$. In the double-exchange (DE) mechanism, there is a density of $(1-x)e_g$ electrons per unit cell, which are free to move through the crystal, subject to a strong Hund's coupling to the localized Mn^{4+} ($S=3/2$) spins. The kinetic (band) energy is optimized by making all the spins parallel. It was predicted to have a fully spin-polarized ground state.[5,6] Among the Ruddelson-Popper series of manganites, (La,Sr)$_{n+1}$Mn$_n$O$_{3n+1}$ ($n=1,2,\infty$), La$_{2/3}$Sr$_{1/3}$MnO$_3$ has the highest T_c and its resistivity is about two orders of magnitude lower than that of the layered manganite ($n=2$) at low temperatures.

The unusual CMR phenomenon defines a basic research problem that involves interplay between the charge, spin, phononic, and orbital degrees of freedom.[7] The vanishing or very small spectral weight at the Fermi level (E_F) and the anomalously broad angle-resolved photoemission spectroscopy (ARPES) features on layered manganites[8,9] suggest a strong electron-phonon coupling and the existence of a pseudogap originated from the formation of charge density wave, which removes at least 90% of the spectral weight at E_F.[9] On the other hand, although less than expected, a finite spectral weight at E_F has been observed in the angle integrated photoemission of three-dimensional (3D) manganites.[10,11] It was speculated that a pseudogap also exists in 3D manganites, but with reduced strength.[8] The first set of ARPES measurements of the low binding energy (E_B) electronic states on La$_{0.66}$Sr$_{0.34}$MnO$_3$ allows us to get de-

tailed information about electronic structure, the Fermi surface (FS), and the evidence of density wave formation on this typical CMR material, to reveal the differet and common features between layered and 3D manganites and to gain an understanding of the anomalous physics of these materials by comparing to prototypical metals in general.

La$_{2/3}$Sr$_{1/3}$MnO$_3$ samples were prepared by growing *in situ* a 1300-Å-thick film heteroepitaxially on a SrTiO$_3$ (001) substrate by an adaptation of pulsed laser deposition.[12,13] *In situ* reflection high-energy electron-diffraction patterns and Kiessig fringes in *ex situ* x-ray reflectivity curves demonstrated that the final film had a surface roughness of less than one monolayer. The stoichiometry was checked *ex situ* using Rutherford backscattering spectrometry and was found to be La$_{0.66}$Sr$_{0.34}$MnO$_3$. Low-energy electron-diffraction analysis showed a clear (1×1) pattern with no sign of surface reconstruction. The transition temperature T_c was determined to be 313 K, lower than the T_c for bulk crystals. The difference in T_c may result from the incomplete relaxation of tensile stress due to the lattice mismatch between the film and the substrate.[14,15] ARPES measurements were performed at the Surface and Interface Spectroscopy (SIS) beamline at the Swiss Light Source (SLS). During the measurements the base pressure always remained less than 1×10^{-10} mbar. The ARPES spectra were recorded with a Scienta 2002 analyzer with an angular resolution of less than 0.2°. Although the best energy resolution is less than 2 MeV, it was relaxed to 40 meV for most measurements to obtain a high photon flux.

Figures 1(a) and 1(b) show normal emission ARPES spectra at 30 K by using circularly polarized light with the propagation vector in the (110) plane and with the photon energy E_{hv} varying from 26 eV to 71 eV, enough for the wave vector **k** to cover the entire Brillouin zone (BZ) along the (001) direction. The spectra show a broad peak on a sloped background, which appears to disperse with E_{hv}. When the incoming light lies in the (100) plane, the dispersion of the broad peak is more clearly visible [Fig. 1(c)]. From the line shape of the spectra it can be seen that (a) in high binding energy scale, when $E_{hv}=38$ eV and 67 eV the position of the dispersive peak is closest to the E_F, and (b) in the low bind-

FIG. 1. (Color) (a) Normal emission ARPES spectra of La$_{0.66}$Sr$_{0.34}$MnO$_3$ at 30 K with photon energy E_{hv} varying from 26 to 71 eV (from bottom to top) with 1 eV step. The corresponding path in the BZ is indicated with a thick line in the drawing between (a) and (b). Spectra corresponding to E_{hv}=38 eV (red), 52 eV (green) and 67 eV (pink) are marked with thicker color lines. (b) Zoom in of the spectra around the spectrum with E_{hv}=38 eV (red) to better view the sharp step near E_F. (c) Normal emission ARPES spectra with E_{hv} varying from 24 to 46 eV (from bottom to top) with 2 eV step. The closed circles indicate the dispersive feature. (d) and (e) The integrated spectral weight over an energy window ± 50 meV centered at E_F. The white (black) color represents high (low) intensity. High symmetry points and directions are indicated by filled circles and axes, respectively. **Q** is the nesting vector.

ing energy scale, the spectra show a clear step at E_F. Centered around two photon energies, E_{hv}=38 eV and 67 eV [highlighted in Fig. 1(a)], the step at E_F sharpens up, clearly indicative of a dispersive "energy band" crossing or reaching the Fermi level and then folding back to below E_F. With the relation of $p=|k_F+G|=0.5123(E_{hv}-\varphi+V_0)^{1/2}$, whereby p is the photoelectron momentum, k_F is the Fermi momentum, G is the reciprocal lattice vector, φ is the work function, and V_0 is the inner potential, we determined V_0-φ=10.16 eV. The near-normal emission spectra (not shown) taken in the same photon energy range with fixed $k_{\parallel}=(\pm0.2,0)\pi/a$ show the same behavior. The dispersion in the high binding energy scale and the step at E_F sharpening up is neither due to the change of the ratio between the photoemission cross sections of the Mn 3d and O 2p subshells, as this ratio increases monotonically when $E_{h\nu}$ varies from 20 to 80 eV, nor due to the 3p-3d resonance of Mn (about 52 eV) since 38 eV is well below the resonance and 67 eV is well above the resonance.

Figures 1(d) and 1(e) show the near- E_F spectral weight measured in the mirror planes (110) and (010). These inten-

sity plots were obtained by first normalizing each individual energy distribution curve (EDC) to its total area and then by integrating the spectral weight over an energy window of ±50 meV centered at E_F. The high intensity straight lines are parallel to the sample surface and situated $\sim0.4\pi/a$ away from Γ_{002} and Γ_{003} in the normal direction. They represent the intersections between the mirror planes and the FS. The FS obtained from the intensity plots is consistent with the observation of the step at E_F sharpening up at E_{hv}=38 eV and 67 eV in normal and near-normal emission, respectively.

We measured ARPES spectra within the mirror plane (010) in a reduced energy range of 24–56 eV. Figures 2(a) and 2(b) show representative spectra with E_{hv}=30 eV, close to the Γ-X in the bulk BZ, and E_{hv}=38 eV, where we found the largest increase at the E_F in normal emission. Except for photon energies close to 52 eV, the other spectra show a similar trend, namely, away from $k_{\parallel}$=0, a broad peak disperses towards lower binding energy, and at about $k_{\parallel}$=0.7π/a the peak no longer disperses and becomes flatter with increasing $k_{\parallel}$. The spectra at E_{hv}=52 eV (not shown) exhibit no clear dispersive features. The spectra at
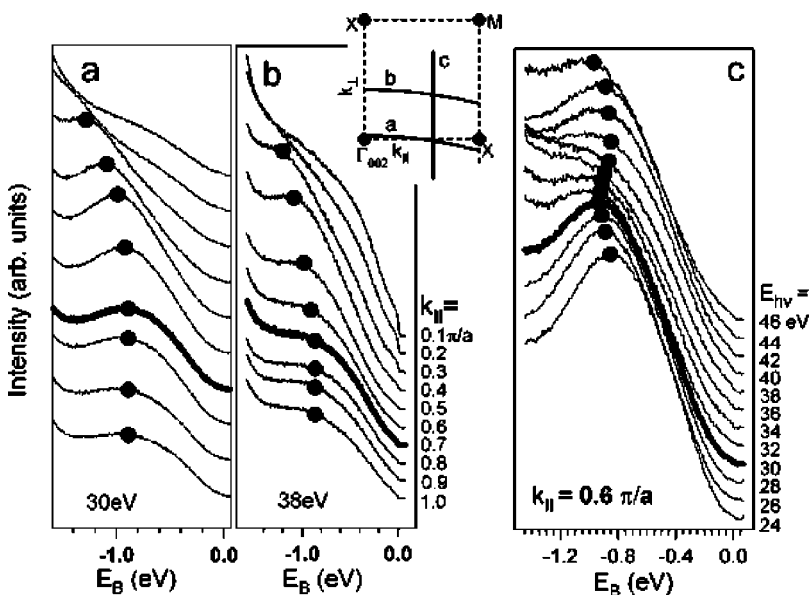

FIG. 2. (a) and (b) ARPES spectra of La$_{0.66}$Sr$_{0.34}$MnO$_3$ at 30 K along the different paths in the BZ [as indicated in the top-right corner of (b)] taken with E_{hv}=30 eV and 38 eV, respectively. (c) ARPES spectra along a path in BZ perpendicular to the sample surface with $k_{\parallel}$=0.6π/a. The spectra were taken with E_{hv} varying from 24 to 46 eV with a 2 eV step. The thick line corresponds the spectrum at the **k** point crossing Γ-X axis.
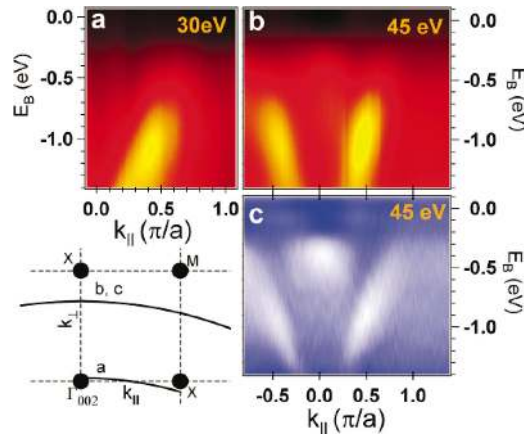
FIG. 3. (Color) ARPES intensity map of $La_{0.66}Sr_{0.34}MnO_3$ at 30 K with $E_{hv}=30$ eV (a) and $E_{hv}=45$ eV (b). The corresponding paths in the BZ are indicated in the bottom-left corner of the figure. (c) The second derivative of EDCs from image (b).

$E_{hv}=38$ eV show a much reduced dispersive peak intensity and the sharp step at E_F persists up to $k_\parallel=0.4\pi/a$, after which the spectral weight at E_F is lost. We also made ARPES measurements with $E_{hv}=38$ eV in off-mirror planes, which contain the surface normal. For this E_{hv} the component of k along the (001) direction is $\sim 0.4\pi/a$ away from Γ_{002}. The obtained spectra have the same behavior as for the (010) mirror plane [Fig. 2(b)] and the sharp step at E_F persists always up to $k_\parallel=(k_x^2+k_y^2)^{1/2}=0.4\pi/a$. Figure 2(c) shows spectra taken along a path perpendicular to the sample surface with a fixed $k_\parallel=0.6\pi/a$. It can be seen that the peak positions are also dispersive, although the dispersion is much weaker than along the sample surface [Fig. 2(a) and 2(b)]. Thus it gives us confidence that the dispersion in Fig. 2(a) and 2(b) is representative of the bulk properties of the sample.

To visualize the dispersion more clearly, we plot the spectral intensity as a function of the wave vector and binding energy in Fig. 3(a) and 3(b) for $E_{hv}=30$ and 45 eV, respectively. Figure 3(c) shows the second derivative of the EDC of the image shown in Fig. 3(b), which enhances the feature close to the center. This feature disperses when E_{hv} changes, but remains nearly nondispersive along $k_\parallel$ for all photon energies.

The first question to answer is why all the ARPES features are anomalously broad. Also, why do they not sharpen up as they approach the Fermi level? It is difficult to describe the features by invoking single quasiparticle excitation, though two other intrinsic phenomena could explain this unusual behavior (1) A single electron cannot be described by an eigenstate: the removal of one electron from the material may be accompanied by other excitations and/or (2) in this system the wave vector is no longer a good quantum number because of some degree of aperiodicity in the crystal.

Similar peak widths have been observed in ARPES spectra of layered magnetoresistive oxides.[8] It was argued that the dispersive peaks should not be thought of as single quasiparticle peaks, but should be considered to be an envelope of many individual peaks resulting from shaking off a certain number of Einstein phonons upon removal of an electron from the system. However, we believe that to explain such anomalously broad ARPES features, other additional effects that involve the ground state of the electronic structure of the system must also be considered.

In conventional band theory, because crystals possess translation symmetry, the electronic states can be represented by the energy band structure $E(k)$. However, if electrons are influenced by an additional nonperiodic potential $\Delta V(\mathbf{r})$, the wave vector k is no longer a good quantum number and cannot fully label the electronic states. In the spirit of disordered alloy theory,[16,17] we can nonetheless still define an energy band, although the system does not possess long-range order, as long as we assume that the energy bands $E(k)$ are complex. This can be physically interpreted by the non-zero imaginary part (E_I) of the energy level representing the disorder-induced broadening of the electronic states by the aperiodic term. In a perfect crystal, E_I vanishes because $\Delta V(r)$ is zero. It should be clear that in general E_I depends on k. $\Delta V(r)$ may be static and/or dynamic. A static perturbation could result from the La/Sr substitution that produces a randomly distributed scattering potential. However, because the low binding energy states are formed by electrons hopping from one Mn site to another via the O $2p$ orbitals, it makes more physical sense to search for the origin of $\Delta V(r)$ in the vicinity of the Mn ions, where the probability of finding charge carriers is high. Concerning the dynamic origin of $\Delta V(r)$, the first candidate would be the distribution of e_g orbitals around a Mn^{4+} ion into which an electron hops from one of the nearest neighbors Mn^{3+}. A temporally varying and locally different orbital distribution around a Mn^{4+} ion (i.e., one with no long-range order) will result in a variation of the hopping amplitude. The second candidate is associated with charge inhomogeneities over one or several lattice spacings, polarons, or clusters.[18] Recent theoretical studies showed that even within the FM phase, which is uniform when time averaged, there is a dynamical tendency towards cluster formation resulting from the net effect of the competition between the DE mechanism and Coulomb interaction.[18] It is reasonable to assume that this kind of nanoscale charge inhomogeneity will perturb the underlying periodic potential and scatter the electrons.

Within the framework of the above arguments, we can now interpret our ARPES spectra in a consistent manner. First, the dispersion of the broad peak up to $k_\parallel \sim 0.7\pi/a$ in the spectra close to Γ-X [$E_{hv}=30$ eV, Fig. 2(a)] represents the trend of the centroid of the energy band, which is associated with the real part of the complex band. However, the peak position results from the convolution of the smearing of the energy band with the incoherent photoemission process. The former results from the finite width, which is determined by the imaginary part of the energy band, and the latter is caused by the shaking off of a certain number of phonons. Above $k_\parallel \sim 0.7\pi/a$, the centroid of the energy band lies above E_F, but again, due to the finite imaginary part, there is still some spectral weight below the Fermi level. Photoemission and the accompanying shaking-off processes are still possible but with less spectral weight, reflected by the reduced peak intensity (flatter ARPES features) and almost no observable dispersion. The same behavior for different spectra along the path parallel to Γ X for different E_{hv} indicates

that the centroids of the energy band cross E_F at more or less the same $k_\parallel$, namely $\sim 0.7\pi/a$. We also performed ARPES measurements with selected E_{hv} in the mirror plane (110). The obtained spectra show a similar trend and the same behavior at $k_\parallel \sim 0.7\pi/a$.

Due to the smearing of the energy band the FS might not be observable in some part of k space. The sharp step at E_F observed in normal and near-normal emission indicates that the smearing of energy levels close to E_F is less pronounced when the energy band disperses in the surface normal direction than in other directions. From the near E_F spectral weight mapped in the mirror planes (110) and (010) [Figs. 1(d) and 1(e)] and the spectra taken at $E_{hv}=38$ eV we have determined flat sections of the FS, which are parallel to the sample surface with $k_\parallel$ extending up to $\sim 0.4\pi/a$. This experimental finding is quite different from the FS predicted by theoretical calculations.[19] The flat portions of the FS and their dense spectral weight at E_F may produce nesting instabilities[20] through a nesting vector as indicated in Fig. 1(d). The folding back of normal and near-normal emission spectra at $k_F=0.4\pi/a$ provides evidence that an incommensurate density wave (e.g., the charge density wave) is formed along the surface-normal direction.[21]

The second question is whether the observed dispersion along the surface and normal to the surface belongs to the same band. Closer scrutiny of the spectra at $E_{hv}=38$ eV [Fig. 2(b)] shows that besides the Fermi step, which starts from $k_\parallel=0$ and persists up to $k_\parallel=0.4\pi/a$, a dispersive feature starting from $k_\parallel=0.3\pi/a$ and dispersing to lower binding energies for larger $k_\parallel$ is clearly visible. The dispersive feature shows the same trend in the spectra taken at $E_{hv}=30$ eV [Fig. 2(a)]. Thus, we believe that dispersions normal to the surface and along the surface result from different bands; one has more one-dimensional (1D)-like character dispersing along the surface normal and located at $k_\parallel < 0.4\pi/a$ in k space, while the other is more two-dimensional (2D)-like, having little dispersion along the surface normal. As no ARPES results on 3D bulk crystal have been reported before, it is difficult to judge the anisotropy in the electronic structure as being a general feature of the 3D La$_{1-x}$Sr$_x$MnO$_3$ in the FM phase or

resulting from incomplete relaxation of the tensile strain in the film. Since the 1D-like band shows a much higher spectral weight around E_F than the 2D band, and the latter is similar to that observed for layered manganites,[8] the finite spectral weight in the 1D-like band might be the origin of the quantitative and qualitative difference between 3D and layered manganites, in particular regarding the T_c and the resistivity dependence on temperature. The finite spectral weight in the 1D-like band might therefore be responsible for the Drude peak found in the optical measurements of 3D manganites,[22] but which was not observed for the layered manganites.[23] In the optical measurements of La$_{0.7}$Sr$_{0.3}$MnO$_3$, the unusual Drude spectrum with an anomalously small spectral weight dominated by an incoherent contribution probably has the same origin as for the smearing of the energy band.

In summary, to account for the anomalously broad ARPES on La$_{0.66}$Sr$_{0.34}$MnO$_3$, we propose that, due to lack of long-range order originating from the random distribution of the orbitals and/or nanoscale charge inhomogeneities, the electronic states should be described by a complex energy band. We believe that many early experimental observations, like the Drude peak in the optical measurements of La$_{0.7}$Sr$_{0.3}$MnO$_3$ (Ref. 22) and the small, but finite spectral weight at E_F in the angle-integrated photoemission spectra of related manganites[10,11] can be attributed to the finite spectral weight in the observed 1D-like band which shows a clear step at the Fermi level. However, the unusual behavior, e.g., the very small Drude weight compared to the dominant incoherent part can be explained by smearing of the complex energy band. The flat portion of the Fermi surface of the 1D-like band should be responsible for the nesting instabilities, which are reflected by the folding back of this band at E_F.

[1] R. M. Kusters *et al.*, Physica B **155**, 362 (1989).

[2] S. Jin *et al.*, Science **264**, 413 (1994).

[3] A. Urushibara *et al.*, Phys. Rev. B **51**, 14103 (1995).

[4] J. Hemberger *et al.*, Phys. Rev. B **66**, 094410 (2002).

[5] N. Furukawa, J. Phys. Soc. Jpn. **63**, 3214 (1994).

[6] J.-H. Park *et al.*, Nature (London) **392**, 794 (1998).

[7] Y. Tokura, Phys. Today **56** (7), 50 (2003).

[8] D. S. Dessau *et al.*, Phys. Rev. Lett. **81**, 192 (1998).

[9] Y.-D. Chuang *et al.*, Science **292**, 1509 (1999).

[10] T. Saitoh *et al.*, Phys. Rev. B **51**, 13942 (1995).

[11] J.-H. Park *et al.*, Phys. Rev. Lett. **76**, 4215 (1996).

[12] P. R. Willmott and J. R. Huber, Rev. Mod. Phys. **72**, 315 (2000).

[13] P. R. Willmott, R. Herger, and C. M. Schlepütz, Thin Solid Films **453-454**, 438 (2004).

[14] W. Prellier, Ph. Lecoeur, and B. Mercey, J. Phys.: Condens. Matter **13**, R915 (2001).

[15] A. Barman and G. Koren, Appl. Phys. Lett. **77**, 1674 (2000).

[16] G. M. Stocks and H. Winter, in *The Electronic Structure of Complex Systems*, edited by P. Phariseau and W. M. Temmerman (Plenum Press, New York, 1984), p. 463.

[17] L. Schwartz, in *Excitations in Disordered Systems*, edited by M. F. Thorpe (Plenum Press, New York, 1982), p. 177.

[18] A. Moreo, S. Yunoki, and E. Dagotto, Science **283**, 2034 (1999).

[19] W. E. Pickett and D. J. Singh, J. Magn. Magn. Mater. **172**, 237 (1997).

[20] G. Gruener, in *Density Waves in Solids*, edited by D. Pines, in Frontiers in Physics, Vol. 89 (Addison-Wesley, Reading, MA, 1994).

[21] J. Voit *et al.*, Science **290**, 501 (2000).

[22] Y. Okimoto *et al.*, Phys. Rev. B **55**, 4206 (1997).

[23] T. Ishikawa *et al.*, Phys. Rev. B **62**, 12354 (2000).